Turkish J. Eng. Env. Sci.
36 (2012) , 19 – 31.

doi:10.3906/muh-1011-22

Static and dynamic bearing capacity of strip footings, under variable repeated loading

Mohammad Reza ARVIN[1,*], **Faradjollah ASKARI**[1], **Orang FARZANEH**[2]
[1] *Geotechnical Earthquake Engineering Department, International Institute of Earthquake Engineering and Seismology, Tehran-IRAN*
e-mails: m.r.arvin@gmail.com, askari@iiees.ac.ir
[2] *School of Civil Engineering, Engineering Faculty, Tehran University, Tehran-IRAN*
e-mail: ofarzane@ut.ac.ir

Received: 29.11.2010

Abstract

The problem of bearing capacity of strip footings is one of the basic and classical problems of geotechnical engineering. Footings under variable repeated loads are vulnerable to collapse due to accumulation of plastic strains or inadaptation. Unlike common limit state methods, the shakedown method can be applied to investigate the behavior of structures subjected to loads varying and repeating in time. In the present study, shakedown theory is employed to determine the static and dynamic bearing capacity of strip footings under variable repeated loads. Effects of load variation and repetition on bearing capacity of footing are studied thoroughly for both static and dynamic loadings. The results indicate that the dynamic bearing capacity of footings is sensitive to dynamic properties of load and subsoil. In addition, results are compared to the bearing capacity of a footing obtained by the common limit state methods.

Key Words: Bearing capacity, footing, shakedown, repeated variable load

1. Introduction

Bearing capacity of strip footings is one of the classical problems in geotechnical engineering. Strip footings are used in a variety of fields such as wall foundations, offshore platforms, and machinery foundations. So far, the footings under monotonic loading have been the subject of many studies. However, bearing capacity of footings under loads varying and repeating in time rarely has been a subject of interest.

When structures are subjected to variable repeated loadings, they might fail due to loads much smaller than the collapse load. That is, load repetition leads to accumulation of plastic strains or low cycle fatigue, which in turn will give rise to the collapse of structures. This phenomenon is referred to as non-adaptation.

Usually, the path and time history of loads that are possible to be applied on a certain structure are unknown. However, a load domain (Δ) in the load space can be defined for the structure so that all probable loads lie inside or on its boundaries.

*Corresponding author

There is a portion of the aforementioned domain under which the structure first shows some plastic strains but subsequently starts to behave elastically with the progression of load application. This phenomenon is called shakedown and the resulting load domain ($\lambda\Delta$) is known as shakedown load domain. The actual load domain Δ and the corresponding shakedown load domain $\lambda\Delta$ are shown in Figure 1 for the case of 2-dimensional load space (F1 and F2).

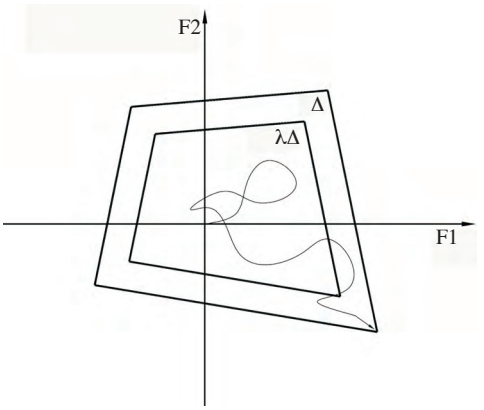

Figure 1. Load domain (Δ) and shakedown load domain ($\lambda\Delta$).

With regards to definition, when the structure shakes down, plastic strains cease to develop and the structure will come back to its previous shape after load application. In that regard, the shakedown load domain of footings under repeated loads can be interpreted as the footing's safe bearing capacity.

Static shakedown theory was first introduced by Melan (1938) for structures under static loading. Koiter (1960) developed kinematic shakedown theory for static loading. Dynamic shakedown was pioneered by Ceardini (1969) for structures subjected to inertial variable loading. Maier (1969), utilizing finite element method and linear programming, converted shakedown theory to an optimization problem for which the objective function is the load factor. Unlike discrete structures, application of shakedown theory in the geotechnical area was restricted to a few studies for years. The first serious work can be attributed to Sharp and Booker (1984), who found the shakedown limit loads of pavements under traffic loads. Using triangular elements separated from each other by discontinuity lines, Bottero et al. (1980) developed an effective numerical approach to obtain the bearing capacity of shallow foundations by limit analysis method.

Later, the method of Bottero et al. was extended by Hossain and Yu (1996) and Yu and Hossain (1998) to the shakedown problem of road pavements. Shiau (2001) solved the problem of 2- and 3-dimensional pavements under traffic loads by both linear programming and nonlinear programming methods. Shiau's formulations for 2D analysis are quite similar to that of Yu and Hossain (1998). Foundation shakedown of offshore platforms under vertically applied dynamic loads was studied by Haldar et al. (1990), using upper bound shakedown theory. However, their research was concentrated on the effect of pore water generation due to shakedown of the footing-soil system. Faria (2002) studied foundation shakedown of an offshore platform under combined static loads.

The present study aims to investigate the vertical bearing capacity of strip footings under 2 different cases of statically and dynamically applied loads. Lower bound static and dynamic shakedown theories are employed to find the solutions. The numerical method of Yu and Hossain (1998) is employed for the static part of the study and is extended for dynamic shakedown analysis.

2. Shakedown theory

The lower bound static shakedown theorem states that:

Shakedown will occur, if a (constant) selfstress state σ^r exists such that superposition of this state and the elastic response to the given loading program at all elements and instants leads to stresses below the yield limit (Maier, 1969).

The lower bound dynamic shakedown theorem states that:

If a fictitious response $u_i^*(x,t)$, $\varepsilon_{ij}^*(x,t)$, $\sigma_{ij}^*(x,t)$ (displacement, strain, and stress, respectively) and a time independent residual stress field $\sigma_{ij}^r(x)$ can be found such that:

$$f\left(\sigma_{ij}^*(x,t)+\sigma_{ij}^r(x)\right)\leq 0 \tag{1}$$

then shakedown will happen at a real response (Ceradini, 1980).

A fictitious response is any elastic solution of systems due to external repeated actions including external forces and strains. It is called fictitious firstly because it is purely elastic and secondly is not obtained necessarily for the real initial conditions. The real response is what actually happens for the systems in reality under variable repeated loads.

If the structure proves to shake down for a specified load domain Δ (Figure 1), then it is safe against any arbitrary variation of load inside and on the load domain.

Based on the forgoing theories, the problem of shakedown can be reduced to an optimization process for which the object is the maximum portion of external actions ($\lambda\Delta$ in Figure 1) that develops an elastic stress field and the variables are the best time independent residual stress field and shakedown factor (Δ). The preceding discussion can be stated in mathematical form as:

$$\lambda=\max\left\{\alpha\;\middle|\;\begin{array}{l} f\left(\alpha\,\sigma_{ij}^*(x,t)+\sigma_{ij}^r(x)\right)\leq 0 \\ \sigma_{ij,j}^r=\text{non}-\text{repeated actions in domain} \\ \sigma_{ij}^r.n_j=\text{non}-\text{repeated actions on free boundaries}\end{array}\right\} \tag{2}$$

In the present study the method of Yu and Hossain (1998) is employed and extended to dynamic shakedown as a solution to Eq. (2).

3. Numerical approach

Based on Eq. (2), the numerical process to find the shakedown solutions consists of 3 fundamental stages.

1. A purely elastic-dynamic analysis of system under dynamic loadings to obtain a fictitious response.
2. Developing equilibrium and yield constraints.
3. Optimization to find the best residual stress field and maximum load factor.

To achieve the second and third steps of the above schedule, the method of Yu and Hossain (1998) was employed with some modifications to make it appropriate for dynamic shakedown analysis. A computer program was developed by the authors to do all the 3 steps discussed above.

In the following section the numerical approach to find shakedown limit and the corresponding computer program will be discussed in brief. Details can be seen in Yu and Hossain (1998).

3.1. Elastic response

A rigid and smooth strip footing resting on a homogeneous half space is supposed to bear the variable vertical loads. The width of the footing assumed to be 1 m (Figure 2).

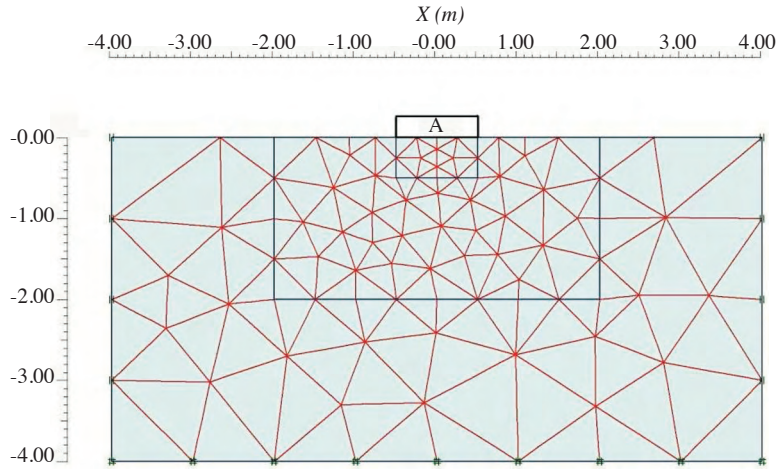

Figure 2. Typical geometry and finite element mesh utilized in this study (Plaxis).

Based on the shakedown theories, a purely elastic analysis needs to be performed to find the elastic stress field. The equation that governs the elastic-dynamic behavior of a system under seismic loads is of the following form.

$$M\ddot{u} + C\dot{u} + Ku = -M\ddot{X}_g \tag{3}$$

where M, C, and K represent mass, damping, and stiffness matrix, respectively, and $\ddot{X}_g$ is the ground acceleration.

The body is discretized into rectangular finite elements (Figure 2). Since linear programming was employed to optimize the results, to ensure linear distribution of elastic stresses through elements, 6-noded rectangular elements and quadratic distribution of elastic displacement were considered for the elastic analysis. For convenience, the mesh generation ability of Plaxis software was utilized. Boundaries are taken far enough in order to avoid the effects of boundaries on the results. For the particular case of rigid smooth footing, the footing is not required to be modeled itself. Instead the true boundary conditions must be considered at the soil-footing interface (Potts and Zdravcovic, 1999, 2001); that is all nodes underneath the base move vertically by the same amount. To do so, the vertical degrees of freedom of base nodes are tied to the center node (point A in Figure 2) (Potts and Zdravcovic, 1999, 2001). Moreover, base nodes are free to move horizontally due to the smoothness of the footing. The load is applied as a unit point load on the center node of the base. For elasto-dynamic analysis, Rayleigh damping is considered for simplicity. That is, damping is the linear combination of stiffness and mass matrix or $C = \eta M + \zeta K$, where C is damping matrix and η and ζ are constant coefficients, obtained by considering the first and second frequency of the soil mass.

The implicit time integration method of Newmark (Bathe, 1982) was employed to find the solution of Eq. (3). Finally, elastic stresses at the corner nodes of the elements were obtained and used in the optimization process.

3.2. Residual stress field

The same finite element mesh used in elastic analysis is considered for residual stress field but here each element has its own node numbers not common to adjacent elements (Figure 3). Every node of an individual element produces 3 unknown stresses σ_x^r , σ_y^r, and τ_{xy}^r. To have a more realistic residual stress field, stress discontinuity lines are adopted between adjacent elements (Figure 3).

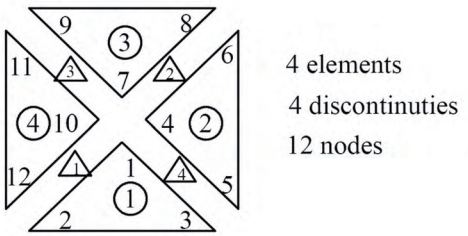

Figure 3. Triangular elements, their node numbering, and stress discontinuities between them (Shiau, 2001).

The optimization comprises equality and inequality constraints. Three types of equality constraint must be satisfied. Firstly equilibrium equations at each element, secondly stress discontinuity requirement at discontinuity lines, and thirdly compatibility of external and internal stresses on free boundaries. Moreover, based on the inequality constraints, the superposition of the elastic stresses (multiplied by shakedown factor) and the residual stresses must be inside or on the yield surface.

The linearization of equilibrium equations for a plane strain element with 3 corner nodes and sign convention, as shown in Figure 4a, leads to the following equation:

$$A_{equil}^{e}\,\sigma^{re} = b_{equil}^{e} \tag{4}$$

where A_{equil}^{e} is a 2×9 matrix with known components. For each element, Eq. (4) creates 2 equality constraints.

To find a more accurate residual stress field, stress discontinuity lines are taken between adjacent elements (Figure 4b). To have a statically admissible discontinuity, the stress components that are normal and tangential

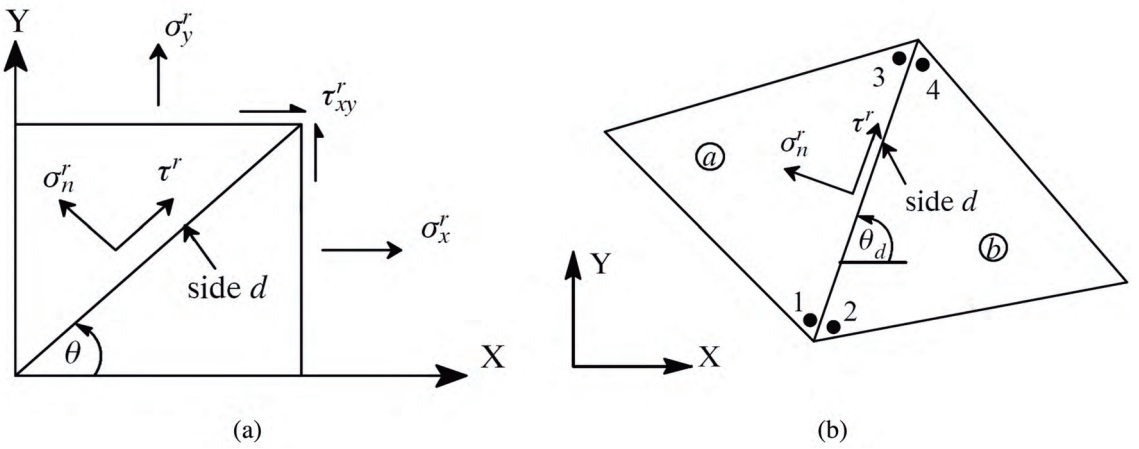

Figure 4. (a) Normal and shear stresses acting on a plane. (b) Residual stress discontinuity between adjacent triangular elements a and b (Shiau, 2001).

to discontinuity edges and common to adjacent elements must be in equilibrium. There is no restriction on the normal stress parallel to the discontinuity line (Figure 4b).

Transformation of stresses onto the discontinuity lines will result in

$$A^d_{dis}\sigma^{rd} = b^d_{dis} \tag{5}$$

where A^d_{dis} is a 4 $\times$ 9 known matrix. Thus, each discontinuity line forms 4 equality constraints.

Equilibrium must be satisfied on the free boundaries of the system (Figure 5).

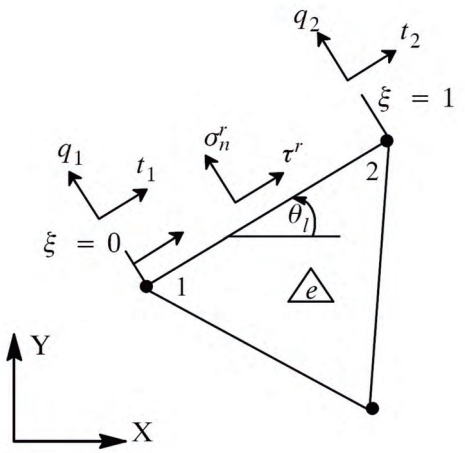

Figure 5. Stress boundary conditions and external stresses acting on free boundary of element e (Shiau, 2001).

Because internal stresses are assumed to vary linearly along the edge of elements, they can be linked to external stresses according to

$$\sigma^r_{n1} = q_1 \ ; \ \sigma^r_{n2} = q_2 \ ; \ \tau^r_1 = t_1 \ ; \ \tau^r_2 = t_2 \tag{6}$$

It should be noted that to derive the Eq. (8), external stresses on the boundaries are assumed to be linearly distributed. Equilibrium of internal and external stresses can be simplified as

$$A^l_{bound}\,\sigma^{rl} = b^l_{bound} \tag{7}$$

where A^l_{bound} is a 4 $\times$ 6 matrix with known arrays.

It is evident from Eq. (7) that a boundary line produces 4 extra equality constrains.

The Mohr-Coulomb yield surface can be approximated by an interior polygon with p vertices and p sides as shown in Figure 6. The criterion of not violating the yield condition may be mathematically imposed on the linearized yield surface. The results according to Sloan (1988) are

$$A_k\,\sigma_x + B_k\,\sigma_y + C_k\,\tau_{xy} \ \leq \ D_k \tag{8}$$

where A_k, B_k, C_k, and D_k are known coefficients associated with kth failure mode (Figure 6).

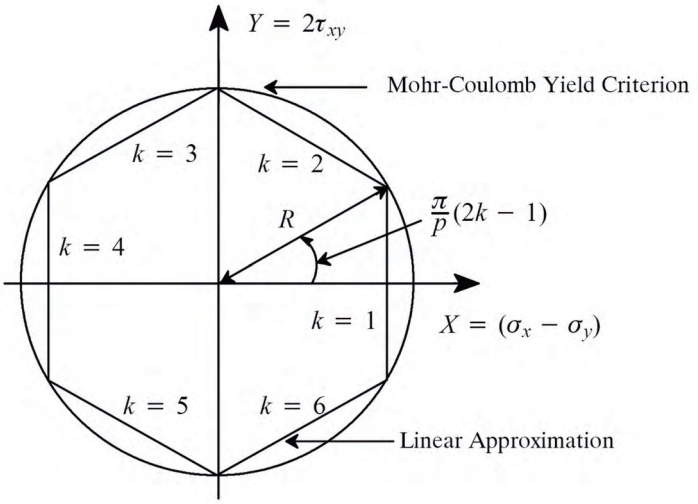

Figure 6. Linearized Mohr-Coulomb yield surface (Shiau, 2001).

Both the residual and elastic stresses are assumed to vary linearly through the elements. Therefore, the yield condition is satisfied for the whole body provided that it is satisfied at the corner nodes of each element.

If combined residual and elastic stresses at the shakedown state $\left(\sigma_{ij} = \sigma^r_{ij} + \lambda\sigma^E_{ij}\right)$ are replaced with the general stress in Eq. (8), then the nonequality constraint of yield will be as follows:

$$A_k\sigma^r_x + B_k\sigma^r_y + C_k\tau^r_{xy} + E_k\lambda \leq D \quad ; \quad k = 1, 2, 3, ..., p \tag{9}$$

where

$$E_k = A_k\sigma^E_x + B_k\sigma^E_y + C_k\tau^E_{xy} \tag{10}$$

For each corner node i of an arbitrary element, Eq. (9) can be written in matrix form as

$$A^i_{yield}\,\sigma^{ri} \leq b^i_{yield} \tag{11}$$

where A^i_{yield} is a $p \times 3$ matrix with known arrays so that it forms p inequality constraints for each node.

Stability requires the yield condition to be satisfied at every point of the system after removal of repeated dynamic loads. That is, the residual stresses need to be inside the yield surface, or

$$A_k\sigma^r_x + B_k\sigma^r_y + C_k\tau^r_{xy} \leq D \quad ; \quad k = 1, 2, 3, ..., p \tag{12}$$

Because dynamic loads are represented as load time histories (here, the acceleration time history), the corresponding stresses are also obtained as stress time histories. An evident solution might be satisfying Eq. (9) at every point and for the entire time history of stresses, which is clearly a cumbersome and time-consuming task. Based on Eqs. (9) and (12), for each dynamic time step and at each element node, $2p$ yield constraints must be taken into account. For a system with E number of elements under a dynamic load with S time steps, the yield criteria add $6pES$ inequality constraints to the optimization procedure.

According to Maier (1969, 1979), the time variable may be eliminated if the maximum components of stress along normals to the yield surface and over the whole time history are considered. In other words, the optimization procedure proposed in Eq. (2) will be reduced to

$$M(x) = \max\left(N\,\sigma^{*}_{ij}\,(x,t)\right)$$
$$\lambda = \max\left\{\alpha \;\middle|\; \begin{array}{l} f\left(\alpha\,M + \sigma^{r}_{ij}\,(x)\right) \le 0 \\ \sigma^{r}_{ij,j} = \text{ non} - \text{repeated actions in domain} \\ \sigma^{r}_{ij}.n_j = \text{ non} - \text{repeated actions on free boundaries} \end{array}\right\} \tag{13}$$

In Eq. (15), N is the normal vector to the yield surface. Based on the first part of Eq. (13), the yield constraint in Eq. (9) may be rewritten as

$$\begin{array}{l} A_k\sigma^{r}_{x} + B_k\sigma^{r}_{y} + C_k\tau^{r}_{xy} + M_k\,(x)\,\lambda \le D; \quad k = 1,2,3,.....,p \\ M_k\,(x) = \max\left(A_k\sigma^{E}_{x}\,(x,t) + B_k\sigma^{E}_{y}\,(x,t) + C_k\tau^{E}_{xy}\,(x,t)\right) \end{array} \tag{14}$$

Because the time variable was eliminated in Eq. (14), the number of yield constraints is reduced from $6pES$ to $6pE$.

3.3. Optimization process

Assembling equality and non-equality constraints discussed in section (3-2), the optimization procedure can be summarized into the following compact form:

$$\begin{array}{ll} Minimize & -\lambda \\ subject & A_1\;X = b_1 \\ & A_2\,X \le b_2 \end{array} \tag{15}$$

where λ is the shakedown safety factor and A_1 and A_2 are equality and in-equality matrices respectively. b_1 and b_2 are given vectors. To see more details, refer to Yu and Hossain (1998).

Because both objective function and constraints are of linear form, Eq. (15) can be solved by linear programming. Here the simplex method is used to find the optimum results.

4. Numerical results

4.1. Statically applied load

A unit vertical load was applied on the footing for the shakedown static analysis so that the resulting load coefficient (λ) would indicate directly the footing bearing capacity. Then the elastic stress field was obtained, performing an elastic dynamic analysis. Subsequently, employing the numerical method discussed in section 3, the best residual stress field and shakedown factor were obtained. The results are presented in dimensionless parameter $\lambda P/c$, in which λ is the shakedown factor, P is the applied load (here is equal to unity), and c is the soil cohesion. In the particular case of weightless soil, $\lambda P/c$ obtained by the shakedown method may be compared to N_c or cohesion factor found by limit load approaches. The elastic limit of the system of footing and underlying soil can be found merely by the method used to find the shakedown limit, assuming zero residual stress field.

An adequate comparison can be made between the value of N_c (the well-known cohesion factor by limit load methods) in different internal friction angles analyzed by the shakedown method, at elastic limit and at collapse limit, respectively. The results are shown in Figure 7.

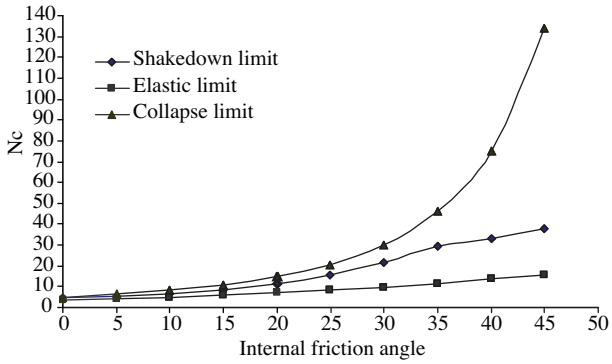

Figure 7. Nc values vs. internal friction angle for elastic, shakedown, and collapse limits.

As Figure 7 shows, the difference between the results of shakedown limit and those of collapse limit increases with the rise in friction angle (up to 112% for $\phi = 45°$). This indicates that care must be taken in the design of footings lying on sandy soils.

4.2. Dynamically applied load

According to the shakedown criterion, the footing is safe if it finally settles to elastic state against a repetitive prescribed dynamic load. In general situations, when the time history of dynamic load repetition is unknown, the dynamic load may be conceived as an inertial load repeated virtually in time. An imaginary sufficient time between 2 subsequent loadings is assumed during which motion caused by the previous loading ceases to develop due to material damping (Figure 8)

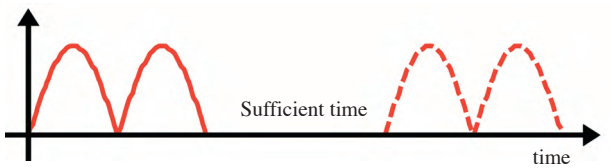

Figure 8. Two successive half-sine loads (solid line) and imaginary reloading (dashed line) considered to evaluate dynamic shakedown limit load of footing in this study.

For the present study, as shown in Figure 8, vertical dynamic loading is considered as a number of successive half-sine loads, applied on the center of footing. The peak value of load is equal to unity.

The number and period of the load for each loading can be different and depend on the situation. Some typical loads employed herein are shown in Figure 9.

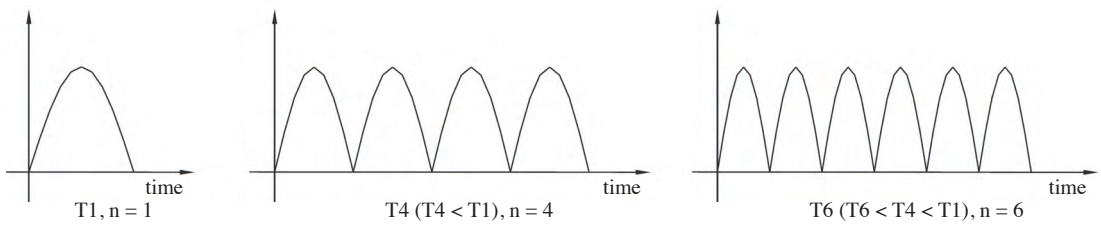

Figure 9. Half-sine loads with different period and number of successive application employed in the present study.

As the vibration properties of the soil are to be taken into account, a wide variety of soil shear modulus and corresponding dominant period of the soil media (T_s) underneath the footing has been considered (Table). Furthermore, half-sine load is applied with different periods (T_m) so that the effect of load dynamic parameters can be examined (Table). Relative period of the system and loading T_s/T_m is a suitable factor to show the dynamic properties of load and subsoil simultaneously. Therefore this ratio was calculated for different T_s and T_m and the results are shown in the Table.

Table. Values of T_s (first column), T_m (first row), and corresponding T_s/T_m employed in the present study.

T_m (s)	0.015	0.02	0.05	0.15	0.3	5	10	30	50
T_s (s)									
0.2702	18.02	13.51	5.404	1.801	0.9	0.054	0.0270	0.009	0.005
0.1709	11.39	8.55	3.418	1.139	0.57	0.034	0.171	0.006	0.003
0.1208	8.05	6.04	2.416	0.805	0.403	0.024	0.012	0.004	0.0024
0.0854	5.69	4.27	1.708	0.569	0.285	0.017	0.009	0.003	0.0017
0.054	3.60	2.70	1.080	0.36	0.18	0.011	0.005	0.002	0.001
0.027	1.80	1.35	0.540	0.18	0.09	.005	0.003	0.0009	0.0005
0.0191	1.27	0.96	0.382	0.127	0.064	0.004	0.002	0.0006	0.0004

In order to ensure that boundaries do not have serious effects on the results, models with different width (W), $\gamma = 20$ kN/m^3, $\phi = 30^\circ$, and damping ratio (DR) equal to 5% were analyzed for varieties of T_s/T_m. The results are depicted in Figure 10. The results were approximated by polynomials of degree 3 for ease of interpretation. The differences between the results of models with $W = 4$ m and $W = 6$ (m) were around 20%, while results of the models with $W = 7$ (m) and $W = 8$ (m) showed only 4% difference on average. There are minor differences (around 2.5% on average) between the results of models with $W = 8$ (m), $W = 9$ (m), and $W = 10$ (m). Therefore, it can be concluded that convergence of results is provided beyond $W = 8$ (m).

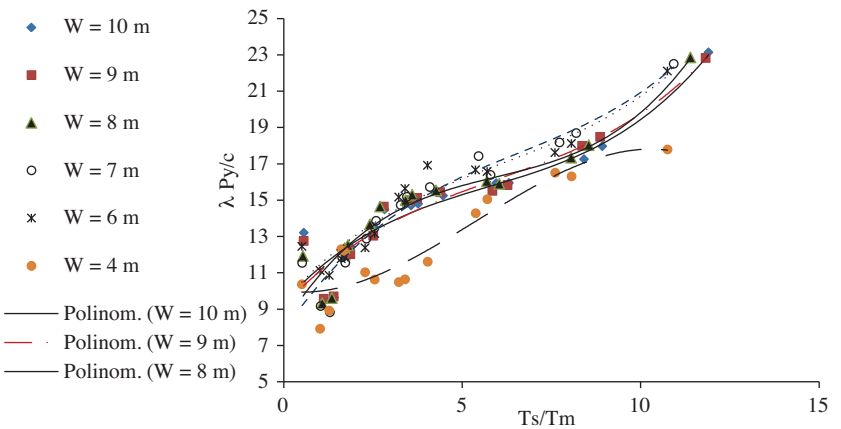

Figure 10. Values of λPy/c for $\gamma = 20$ kN/m^3 , $\phi = 30^\circ$, and DR = 5% for models with different widths (W).

Since increase in the width of the model results in a significant rise in the optimization constraints and time of analyses and due to small differences between the results of models with $W = 7$ (m), $W = 8$ (m), and $W = 9$ (m), the model with $W = 8$ (m) was selected for the analyses (Figure 2).

To study the effect of variations in damping ratio on the results, different values of damping ratio (DR) were considered ($DR = 5\%$, 10%, and 20%). Bearing capacity of the footing resting on soil with $\gamma = 20$ KN/m^3 and $\phi = 10^\circ$ was calculated subsequently against variations in T_s/T_m (Figure 7).

As Figure 11 shows, regardless of the value of DR, bearing capacity ($\lambda P/c$) decreases with increase in T_s/T_m and then starts to rise. The minimum bearing capacity is obtained around $T_s/T_m = 1$, which clearly depicts the effect of resonance in weakening the footing.

Values of static bearing capacity for the same problem are depicted in Figure 11 as well. As seen, static bearing capacity is constant with variation in T_s/T_m. In other words, bearing capacity calculated by static analysis is not able to account for the dynamic properties of load and subsoil and might be underestimated where it is greater than the corresponding dynamic one in low values of T_s/T_m and is highly conservative at large values of T_s/T_m (Figure 11).

Damping as a dynamic factor is seen to have an increasing effect on bearing capacity, especially at higher values of T_s/T_m (Figure 11).

To examine the effects of load number on the results, half-sine load for different number of successive applications ($n = 2$, 4, and 10) is enforced on the footing. Soil is supposed to have a friction angle equal to 10°, $DR = 5\%$, and unit weight of $\gamma = 20$ kN/m^3. The results presented in Figure 12 show that load number increase leads to decrease in bearing capacity.

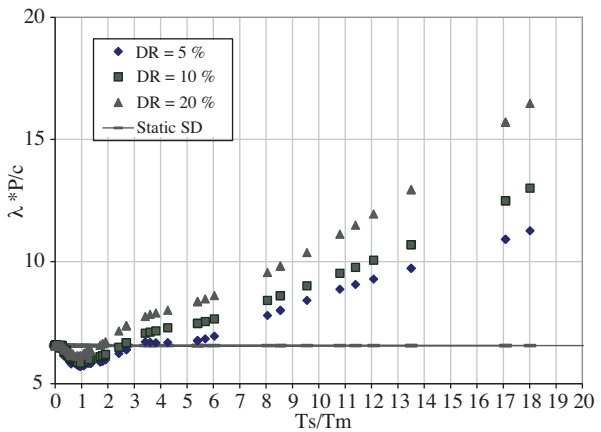

Figure 11. Bearing capacity of footing vs. dynamic parameter (Ts/Tm) in DR = 5%, 10%, 20%, and n = 2 for soil with $\gamma = 20$ KN/m^3 and $\phi = 10^\circ$.

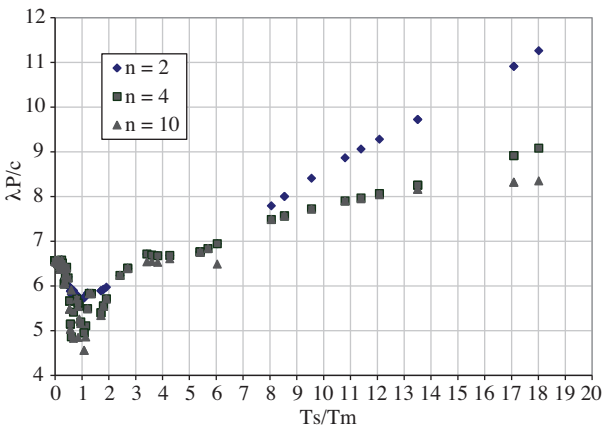

Figure 12. Effect of number of successive half-sine loads on shakedown limit of footing for soil with $\gamma = 20$ KN/m^3, $DR = 5\%$, and $\phi = 10^\circ$.

Effects of internal friction angle on the results were also evaluated by solving some examples. The footing was subjected to sine load with n = 1. Soil was supposed to have $\gamma = 20$ kN/m^3, $DR = 5\%$, and take different values of internal friction angles ($\phi = 10^\circ$, 20°, 30°, and 40°). Variations of $\lambda P/c$ with T_s/T_m for different ϕ are presented in Figure 13.

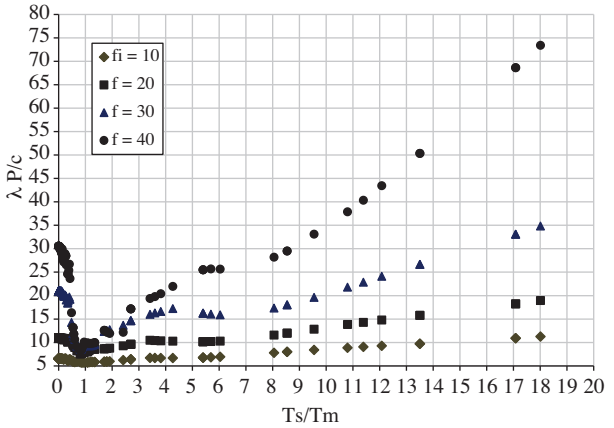

Figure 13. Effects of ϕ on the dynamic bearing capacity of footing under sine load with n = 1 on the soil with γ = 20 KN/m^3 and DR = 5%.

As Figure 13 shows, increase in ϕ results in the growth of $\lambda P/c$, regardless of the value of T_s/T_m. Again, the effect of resonant is evidently observed at $T_s/T_m = 1$, where $\lambda P/c$ takes its minimum value along curves of different ϕ.

5. Conclusions

The vertical bearing capacity of rigid smooth footings subjected to static or dynamic variable repeated loading has been investigated in this study utilizing shakedown theory. An efficient numerical method based on the finite element method and linear programming has been employed by the authors to apply shakedown theories. Footing bearing capacity was calculated against 2 classes of repeated variable loadings, statically applied loads and dynamic sinusoidal loads.

The main conclusions of the present study are as follows:

1. In the case of variable loading, regardless of soil plastic characteristics, the bearing capacity of footing under variable repeated loads is always lower than the ultimate bearing capacity and higher than the elastic limit of footing.

2. Unlike other limit state methods, shakedown theory is able to include dynamic properties of soil and loading in the analysis. Bearing capacity of footing is very sensitive to the value of T_s/T_m, which takes account of the subsoil and load dynamic characteristics. The minimum value of bearing capacity is obtained at $T_s/T_m = 1$, where resonance occurs. For $T_s/T_m < 1$, bearing capacity shows a descending nature and for $T_s/T_m > 1$ exhibits ascending characteristics.

3. The results show that footing bearing capacity by limit state methods is not reliable in the case of variable repeated loading. The ultimate bearing capacity of footing might be lower than the shakedown limit at small values of T_s/T_m and may be larger than the shakedown bearing capacity at higher values of T_s/T_m.

4. Effects of number of successive applications of sine loads, as the representative of dynamic loads, are also studied. The results indicate that increase in load number leads to decrease in footing bearing capacity.

5. Dynamic bearing capacity of footings under variable repeated loads is greatly affected by the change in the internal friction angle of soil. The results show that increase in the soil internal friction angle leads to a rise in the dynamic bearing capacity of footings.

References

Bathe, K.J., "Finite Element Procedure in Engineering Analysis", Prentice Hall, 1982.

Bottero, A., Negre, R., Pastor, J. and Turgeman, S., "Finite Element Method and Limit Analysis Theory for Soil Mechanics Problems", Comput. Methods Appl. Mech. Engrg. 22, 131-149, 1980.

Ceradini, G. "Dynamic Shakedown in Elastic-Plastic Bodies", Journal of Engineering Mechanics Division-ASCE, 106, 481-498, 1980.

Ceradini, G., "Sull'adattamento Dei Corpi Elastoplastici Soggetti ad Azioni Dinamiche". Giorn. Genio Civile, 239-250, 1969.

Faria, P.D., "Shakedown Analysis of Foundation Structures", Methods Neumericos En Ingenieria Y Ciencias Aplicadas, 733-744, 2002.

Haldar, A.K., Reddy, D.V. and Arockiasamy, M., "Foundation Shakedown of Offshore Platforms", Computers and Geotechnics, 10, 231-245, 1990.

Hossain M.Z. and Yu H.S., "Shakedown Analysis of Multi-Layer Pavements Using Finite Element and Linear Programming", Proc. 7th Australia-New Zealand Conference on Geomechanics, Adelaide, 512-520, 1996.

Koiter, W.T., "A New General Theorem on Shakedown of Elastic-Plastic Structures", Proceedings of Koninklijke Nederlandse Akademie van Wetenschappen, B59, 24-34, 1956.

Maier, G., "Shakedown analysis', in 'Engineering Plasticity by Mathematical Programming", Cohn, M.Z., Maier, G., Eds., Pergamon Press, Chapter 6, 107-134, 1979.

Maier, G. "Shakedown Theory in Perfect Elastoplasticity with Associated and Nonassociated Flow Laws: A Finite Element, Linear Programming Approach", Meccanica, 4, 250-260, 1969.

Melan, E., "Der Spanning Zustand Eines 'MisesHenckyschen' Kontinuums Bei Verändlichen Belastung", Sitz. Ber. Akad. Wiss. Wien, Abt. lla, 147, 73, 1938.

PLAXIS (2008).

Potts, D.M. and Zdravcovic, L., "Finite Element Analysis in Geotechnical Engineering, Application", Thomas Telford, 2001.

Potts, D.M. and Zdravcovic, L., "Finite Element Analysis in Geotechnical Engineering, Theory", Thomas Telford, 1999.

Sharp, R.W. and Booker J.R., "Shakedown of Pavements under Moving Surface Loads", Journal of Transport Engineering, ASCE, 110, 1-14, 1984.

Shiau, S.H., "Numerical Methods for Shakedown Analysis of Pavements under Moving Surface Loads" PhD thesis, The University of Newcastle, Australia, 2001.

Sloan. S.W., "Lower Bound Limit Analysis Using Finite Elements and Linear Programming", Int. J. Numer. Anal. Methods Geomech., 12, 61-77, 1988.

Yu, H.S. and Hossain, M.Z., "Lower Bound Shakedown Analysis of Layered Pavements Using Discontinuous Stress Fields", Computer Methods in Applied Mechanics and Engineering, 167, 209-222, 1998.